PULSED IONOSPHERIC CUSP FLOW: SIGNATURE OF ALFVÉN SURFACE WAVE INDUCED RECONNECTION?

P. Prikryl
Communications Research Centre, Ottawa, Canada

G. Provan, K.A. McWilliams and T.K. Yeoman
Department of Physics and Astronomy, University of Leicester, UK

Pulsed ionospheric flows (PIFs) in the cusp footprint are believed to be a consequence of magnetic reconnection on the dayside magnetopause, ionospheric signatures of quasiperiodic flux transfer events (FTEs). However, the question of what causes pulsed reconnection has remained unanswered. Here the PIFs are correlated with Alfvénic fluctuations that were observed in the upstream solar wind. It is concluded that on these occasions the FTEs were pulsed by Alfvén waves coupling to the dayside magnetosphere. The cross-correlation analysis of the IMF and the ground magnetic field near the cusp footprint indicates time lags that are several minutes longer than the propagation time estimates computed from multipoint solar wind measurements. These results suggest a delay between the expected arrival of the Alfvén wave southward turning and the reconnection onset on the dayside magnetopause. We interpret the delay in terms of the intrinsic time scale for reconnection [*Russell et al*., 1997] and the model of surface-wave-induced magnetic reconnection [*Uberoi et al*., 1999]. The latter authors argued that surface waves with wavelengths larger than the thickness of the neutral layer can induce tearing-mode instability giving rise to an intrinsic timescale for the reconnection onset. The timescales inferred from theory are similar to the observed delays.

1 Introduction

The ionospheric dynamics near the cusp footprint attests to the processes at the dayside magnetopause, pulsed magnetic reconnection in particular [*Cowley et al.*, 1991; Lockwood et al., 1993]. Series of quasiperiodic poleward moving auroral forms (PMAFs) at the polar cap boundary [*Vorobjev et al.*, 1975; Sandholt et al., 1990; Øieroset et al., 1997] and pulsed ionospheric cusp plasma flows observed by UHF incoherent scatter [*VanEyken et al.*, 1994], VHF [*Goertz et al.*, 1985] and HF coherent scatter radars [*Pinnock et al.* 1995; Provan et al., 1998] are widely accepted to be ionospheric signatures of pulsed magnetic reconnection. Since *Dungey* [1961] introduced the concept of magnetic reconnection as a steady-state phenomenon in a model of open magnetosphere, the reconnection has become viewed as a time-dependent process resulting in a non-steady ionospheric convection [*Russell,* 1972; *Russell and McPherron*, 1973; Cowley and Lockwood, 1992]. While the early observations by ISEE satellites provided evidence for quasi-steady dayside reconnection [*Paschmann et al.*, 1979] impulsive reconnection of the magnetosheath and magnetospheric fields is regarded as a primary mechanism for magnetic flux transfer from solar wind to the magnetosphere [*Russell and Elphic,* 1978, 1979]. Episodes of such flux transfer that are referred to as flux transfer events (FTEs) occur with separation times between successive FTEs ranging from of a few minutes to several tens of minutes [*Lockwood et al.*, 1989; *Lockwood and*

Wild, 1993; *Kuo et al.*, 1995]. In search for the cause of the pulsed nature of reconnection, *Lockwood and Wild* [1993] suggested that quasiperiodic FTEs could arise from the IMF-B_Z fluctuations while *Le et al.* [1993] argued in favor of spontaneously occurring FTEs. *Kuo et al.* [1995] and *Russell et al*. [1997] concluded that the quasiperiodic occurrence of FTEs is controlled by the magnetopause or magnetosphere.

The observation of delayed appearance of FTEs after the expected arrival time at the subsolar magnetopause of the southward IMF turning lead *Russell et al*. [1997] to suggest that reconnection is not immediately responsive to a southward IMF. They showed that FTEs can be delayed as long as 7 min from the arrival time of the southward IMF at the magnetopause and suggested this to be an intrinsic time scale that is controlled by the magnetopause or the magnetosphere rather than external drivers. More recently, some evidence of solar wind/magnetosheath MHD waves modulating the reconnection rate (as inferred from ionospheric cusp flows observed by SuperDARN) has been found [*Prikryl et al.*, 1998, 1999]. Relatively long (~7 min) delays of the enhanced ionospheric flows after the southward turning of the IMF in the postnoon magnetosheath were observed [*Prikryl et al.,* 1998].

Solar wind plasma is highly structured and turbulent medium supporting a variety of MHD modes. Alfvén waves are commonly observed [*Belcher and Davis,* 1971], particularly in high-velocity solar wind streams. The observations [Sibeck et al., 1997, 2000] and MHD modeling [*Lin et al.,* 1996, *Cable and Lin,* 1998] confirmed previous theoretical work and showed that Alfvén waves interact with the bow shock and fast, intermediate (Alfvén), and slow modes are transmitted into the magnetosheath. In a recent survey of magnetosheath MHD waves *Sibeck et al.* [2000] confirmed theoretical predictions that most of the magnetosheath fluctuations originate in the solar wind and showed that the antisunward propagating Alfvénic fluctuations in the solar wind generate antisunward and sunward propagating (but not strictly Alfvénic) fluctuations in the magnetosheath. Because the amplitudes of the observed velocity fluctuations were depressed by about a factor 5 or less with respect to the predicted amplitudes for Alfvénic fluctuations, and antiphase density and magnetic field magnitude perturbations were present, they attributed these fluctuations to slow mode waves.

Here we use the solar wind, HF radar and ground-based magnetometer data to examine correlations between the Alfvénic fluctuations and pulsed ionospheric flows (PIFs) in the cusp footprint. The observed cross-correlation lags are compared with estimated propagation times between the spacecraft and ionosphere.

2 Instruments and techniques

The CUTLASS bistatic radar (with stations in Finland and Iceland) is a part of the extended international network of HF radars called SuperDARN (Super Dual Auroral Radar Network) [*Greenwald et al.*, 1995]. Each radar is a frequency agile (8-20 MHz) radar forming 16 beams of azimuthal separation of 3.24^o, gated into 75 range bins (45 km long in standard operations when the dwell time for each beam is 7 s giving a full scan over 52^o in azimuth usually every 2 min). Several parameters including the line-of-sight (l-o-s) Doppler velocity, spectral width and backscatter power from ionospheric plasma irregularities are routinely measured. In the standard mode the velocity that was measured by two radars can be combined to provide convection velocity perpendicular to the magnetic field.

Ground-based magnetometer data from the IMAGE array [*Viljanen and Häkkinen,* 1997] are used to support the SuperDARN data. The International Solar-Terrestrial Physics (ISTP)/ Global Geospace Science (GGS) mission includes the WIND spacecraft [*Ogilvie and Parks,* 1996] with instruments that

included the Magnetic Fields Investigation (MFI) and 3-D Plasma (3DP). Additional data from solar wind and magnetosheath obtain by ACE [*Smith et al.*, 1999] and IMP 8 are used to examine the spatial coherence of solar wind structure and to measure propagation delays between the spacecraft and the ionosphere.

3 Observations

It is well known that the magnetic reconnection rate at the magnetopause subsolar point increases when the IMF turns southward (antiparallel merging) [*Rijnbeek et al.,* 1984, *Berchem and Russell*, 1994]. The newly opened field lines are subject to a curvature force (magnetic tension) and as they are straightened and dragged antisunward by solar wind the ionospheric plasma at the cusp footprint moves with them resulting in enhanced flows that can be observed by SuperDARN radars [*Pinnock et al.,* 1995]. If the IMF fluctuates (B_Z in particular) so does the reconnection rate and the ionospheric flow in the cusp footprint. If the IMF fluctuations are due to Alfvén waves, one can expect a series of quasiperiodic reconnection pulses evidenced by radar observations of PIFs. The IMF B_Y fluctuations control the cusp (DPY) currents [*Stauning et al.*, 1995] that are associated with poleward progressing ionospheric flows for the IMF $B_Z < 0$. This is demostrated for Alfvén waves observed in the solar wind on May 10, 1998.

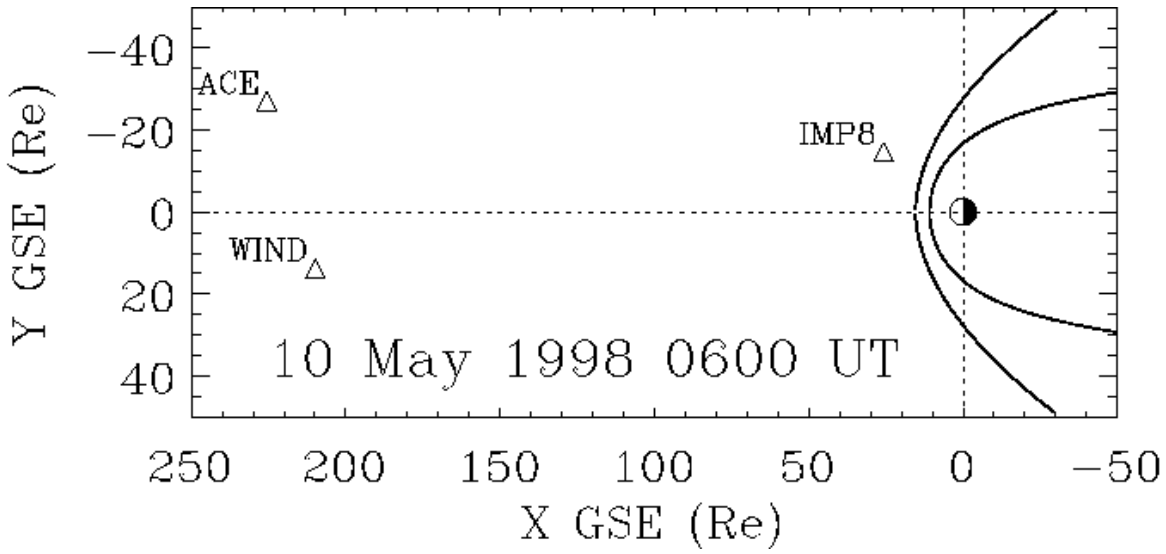

Fig. 1 The ISTP spacecraft positions in GSE coordinates.

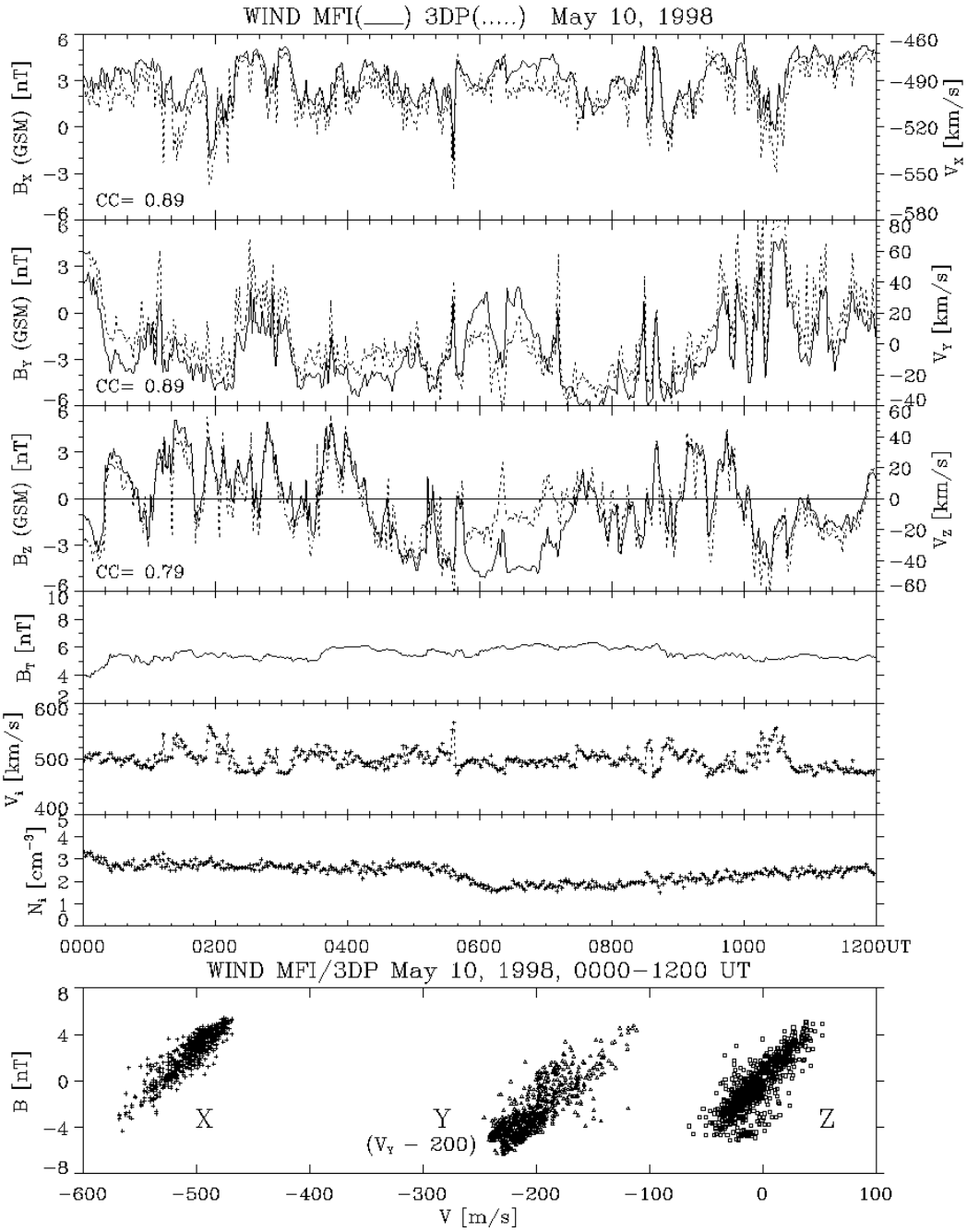

Fig. 2 Alfvénic fluctuations in the solar wind observed by WIND spacecraft on May 10, 1998. The coefficients of correlation between the corresponding components of the IMF (solid line) and ion velocity (dotted line) and scatter plots (bottom) are shown. The IMF magnitude and ion density were relatively constant.

3.1 Case study: 10 May 1998

At 0600 UT, WIND was located at (209.8, 13.7, 29.2 R_E), IMP 8 was at (25.6, -14.7, 14.5 R_E) and ACE at (225.6, -27.0, -19.7 R_E) in GSE coordinates (Figure 1). At these widely separated locations (WIND at 201.2 R_E, IMP 8 at 21.8 R_E and ACE (data not shown) at 217.0 R_E from the magnetopause, respectively) all three spacecraft observed large amplitude Alfvén waves having similar wave forms for many hours. Figure 2 shows the IMF and plasma data from WIND demonstrating the presence of Alfvén waves in the solar wind. The corresponding components of the IMF and ion velocity fluctuations are highly correlated (correlation coeficients and scatter plots are shown) while the IMF magnitude and plasma density remained relatively constant. For sunward oriented background IMF ($B_X > 0$) the positive correlations indicate antisunward propagating Alfvén waves [*Belcher and Davis,* 1971] convected at the solar wind speed of about 500 km/s. Also, we compared the predicted Alfvénic velocity fluctuations obtained from the Walen relation $\Delta\mathbf{V} = \pm\Delta\mathbf{B}/(4\pi\rho)^{1/2}$, where ρ is the plasma mass density, with the observed fluctuations (following *Sibeck et al.* [1997] we assumed that alpha particles constitute 10% of the solar wind number density). The wave forms and amplitudes of the predicted (not shown) and observed velocity fluctuations are very similar confirming the Alfvénicity of the solar wind fluctuations during this time.

High spatial coherence is observed between the spacecraft. The corresponding IMF components measured by WIND, ACE, and IMP 8 (the 15-s IMP 8 magnetic field data are shown in Figure 3a) are correlated and the maximum correlation coefficients and corresponding lags are shown in Table 1 for a 4-hour period. Time series of 1-min averaged and interpolated magnetic field data were used.

3.1.1 Estimate of the spacecraft-magnetopause time lag and correlation between the IMF and ground magnetic field

When estimating propagation delays between a single spacecraft and the subsolar magnetopause a standard approach [e.g., *Lester et al.,* 1993] is to assume that the solar wind disturbance "phase front" is aligned with the mean IMF. We first determine the mean IMF orientation using the angle φ_B between the positive X (earth-sun) axis line and the projection of the magnetic field vector **B** to the XY plane, the **B** inclination θ_B to the XY plane and so-called IMF cone angle α_B between **B** and positive X axis. Broken lines in Figures 3a and 3b (top) show smoothed values of these angles (2-hour smoothing window is used). For a range of α_B values between 55^o and 70^o and the solar wind speed of 500 ± 20 km/s the estimated mean propagation delays between the spacecraft and the subsolar magnetopause [*Lester et al.,* 1993] are 49 ± 3 min, 45 ± 3 min and 4 ± 1 min, for WIND, ACE, and IMP8 respectively.

In reality, the phase fronts are usually not aligned with the mean IMF [*Richardson and Paularena,* 1997]. With 3 spacecraft monitoring the solar wind we can compute [*Nishitani et al.*, 1999] the orientation of the phase fronts (assuming plane wave propagation) by using the correlation lags between pairs of spacecraft (for each pair we take an average of two time lags obtained for the IMF B_Y and B_Z components as listed in Table 1).

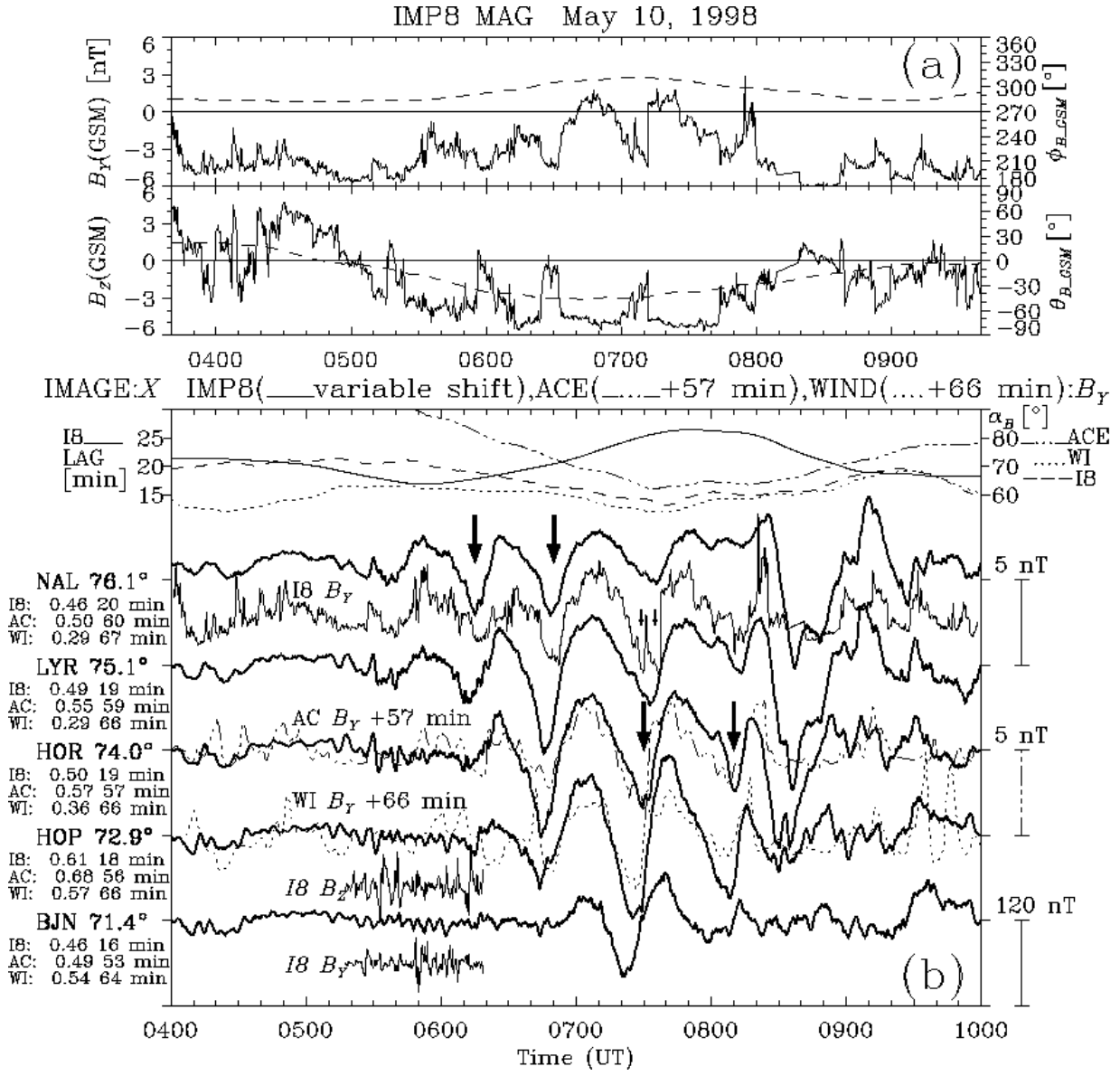

Fig. 3 (*a*) The IMP-8 IMF B_Y and B_Z (solid line) and the mean IMF orientation (broken line). The angle φ_B is between the positive X (earth-sun) axis line and the projection of the magnetic field vector **B** to the XY plane, the **B** inclination θ_B to the XY plane. (*b*) The detrended X-component of the ground magnetic field (heavy line) measured by IMAGE (Svalbard) magnetometer array. The first thin solid line at the top is the variable lag obtained from correlation between the WIND IMF B_Y and NAL X time series using an advancing 1-hour window. Also, the mean IMF cone angle α_B (broken lines) for WIND and IMP8 are superposed. The ground magnetic data plots are interspersed with detrended and time shifted IMF B_Y and B_Z measured by IMP8 (thin solid line) and WIND (dotted line). The detrended and variably shifted WIND IMF B_Y is superposed below the NAL X time series. The maximum correlation coefficients and corresponding average lags are shown. The heavy and light arrows indicate some of the major and minor intensifications of the westward DPY current, respectively.

For the solar wind speed of 500 ± 20 km/s, dynamic pressure of 2 nPa and the average correlation lags measured by three pairs of spacecraft we find the orientation angles of the normal to the phase front (the angle, φ_n, between the normal and the Sun-Earth line in the ecliptic plane and the inclination, θ_n, out of the ecliptic plane) passing the spacecraft by solving equation [*Nishitani et al.,* 1999]:

$$(X_2 - X_1 - V_x\tau)\cos\varphi_n + (Y_2 - Y_1 - V_y\tau)\sin\varphi_n = (Z_2 - Z_1 - V_z\tau)\tan\theta_n \qquad (1)$$

where τ is the time lag between constant phase fronts convected at velocity (V_x ,V_y ,V_z) passing two spacecraft located at (X_1 ,Y_1 ,Z_1) and (X_2 ,Y_2 ,Z_2) in GSE coordinates. For simplicity, we take $V_y = V_z = 0$ (approximately true on average; see Figure 1) and use the mean correlation lag for τ. Figure 4 shows possible orientations of solar wind front (varying φ_n from –90° to +90° corresponding θ_n are calculated) for two spacecraft pairs. The shaded rectangle represents a subrange of values φ_n and θ_n that satisfy the equation for a given range of V_{SW}. Adding one more spacecraft pair (ACE,WIND) we obtain a range of possible angles φ_n = 45 ± 18° and θ_n = –12 ± 22°. Using these values in the algorithm described by *Nishitani et al.* [1999] the estimates of the propagation delay between the spacecraft and the subsolar magnetopause are 50 ± 3 min (WIND), 42 ± 3 min (ACE), and 4 ± 3 min (IMP8). These estimates are similar to those above which are based on the assumption of the phase front alignment with the mean IMF. For propagation in the magnetosheath, a standard approach assuming the gasdynamic *Spreiter and Stahara* [1980] model was used as discussed by *Lester et al.* [1993].

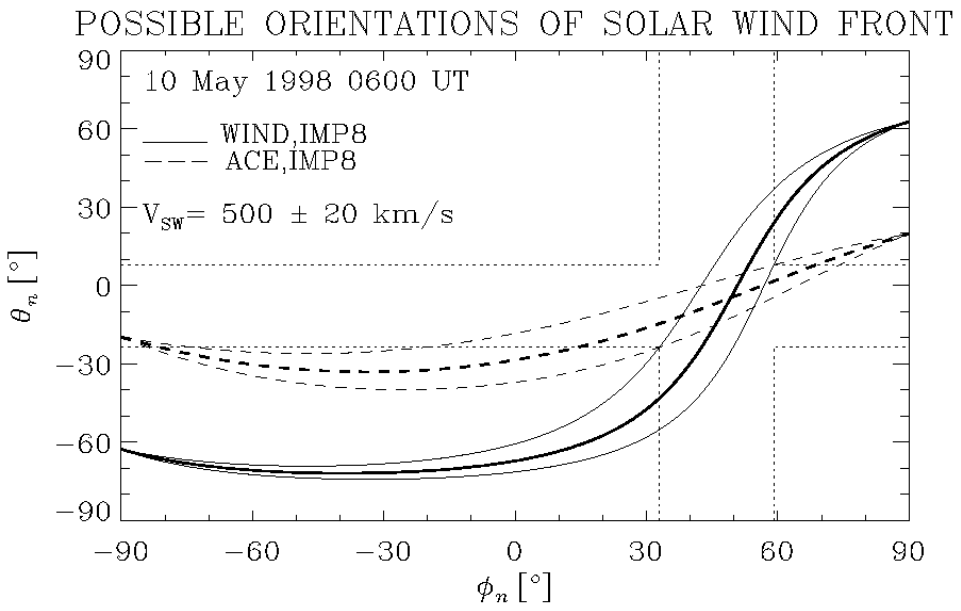

Fig. 4 Possible orientations of solar wind front (varying φ_n from –90° to +90° corresponding θ_n are calculated) for two spacecraft pairs. The shaded rectangle gives a subrange of values for φ_n and θ_n that satisfy the equation (1) for a given range of V_{SW}.

3.1.2. Comparison with the observed cross-correlation lags

Figure 3b shows the detrended time series of the ground magnetic field X component perturbations due to DPY currents measured by the IMAGE (Svalbard) magnetometer array and correlated with the IMF B_Y measured by IMP8 (Figure 3a), ACE and WIND. The overall maximum correlation coefficients and lags (propagation delays between the solar wind and the ionosphere) are shown. The average time lags resulting in maximum correlation coeficients obtained for the cusp portion of the IMAGE array (HOP-NAL) range from 65 to 67 min for WIND, 56-60 min for ACE, and 18 to 20 min for IMP 8 (Table 2). These correlation lags are several minutes longer than the estimated spacecraft-magnetopause time lags discussed above even if one subtracts the Alfvén propagation time (usually a few minutes) to account for propagation between the magnetopause to the ionosphere. From the correlation between the IMF B_Z or the solar wind dawn-dusk (E_Y) component of the electric field ($-\mathbf{V}\times\mathbf{B}$) derived from the WIND MFI/3DP data and the ground magnetic X component 1-3 min shorter correlation lags are found. The dawn-dusk E_Y electric field component (superposed in Figure 5 with a shift of 64 min) fluctuated quasiperiodically with amplitudes up to ±2 mV/m.

The above correlation lags only give average delays of the ionospheric response to the solar wind (long period) driver. In fact, the delays were quite variable over the 6-hour period shown in Figure 3. To examine the delay variability correlation lags were computed for NAL X and IMP8 B_Y time series using 1-hour window that was shifted in 30-min steps. The resulting time series of lags that was interpolated to match the magnetometer sampling rate and then smoothed is shown in Figure 3b (top solid line). These time lags (ranging between 17 and 27 min) are anticorrelated with the mean IMF cone angle suggesting that the lag variation is mainly caused by a variable orientation of the phase front approximately aligned with the mean IMF. The variable time lags obtained from the correlation analysis are used to shift the IMP8 IMF time series in Figure 3b. After the adjustment for the variable delay the IMP8 B_Y trace matches rather well the long period variation of the ground magnetic field at high latitudes. Also, on time scales of minutes, some one-to-one correspondence between the IMF and ground magnetic field fluctuations can be seen, particularly at lower latitudes (see the detrended and shifted section of the IMF B_Y and B_Z time series). The amplitude of short period ground magnetic pulsations that peaked at lower latitudes while the phase progressed poleward suggest field line resonances (FLRs).

3.1.3 Radar observations of PIFs

The long period ground magnetic X component perturbations are due to poleward progressing DPY currents [e.g., *Stauning et al.*, 1995]. For the IMF $B_Y < 0$, and $B_Z < 0$ the intensifications of the Hall current progress poleward and are associated with eastward flow channels. Figure 5 shows the CUTLASS Finland radar latitude-time-velocity (LTV) plots for beams 0, 9, and 13. The dwell time for each beam was 12 s and a full scan took 4 min resulting in lower than standard time resolution. The line-of-sight (l-o-s) velocity is color coded with negative velocities indicating motions away from the radar, while grey indicates ground scatter. It was only after the ambient IMF and solar wind electric field turned southward and duskward, respectively, that a significant merging occurred at the subsolar point as evidenced by long period (30-40 min) PIFs observed by the radar

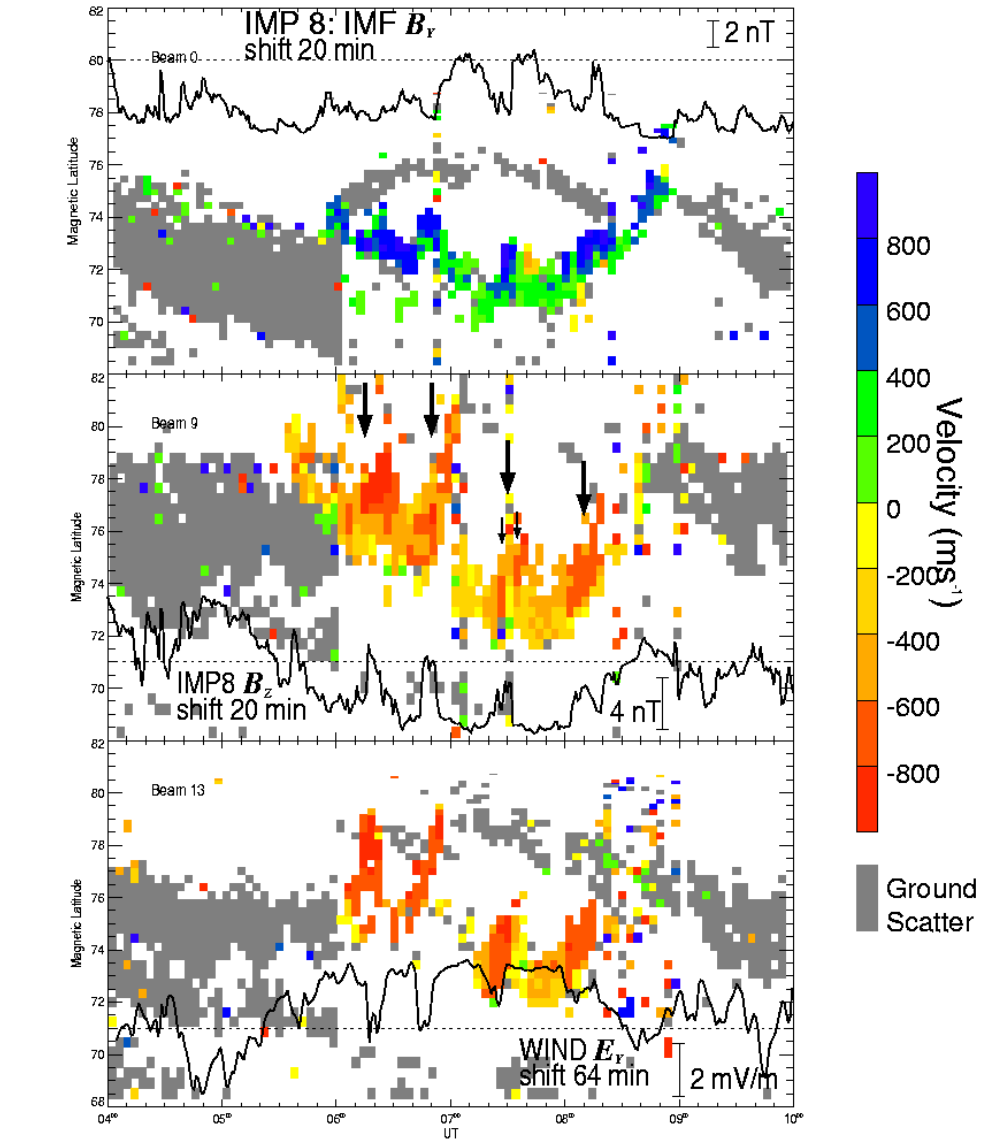

Fig. 5 The Finland radar (beams 0, 9, and 13) color-coded line-of-sight velocity showing quasiperiodic poleward progressing flow bursts (PIFs) associated with DPY current intensifications (arrows from Fig. 3b). Shifted time series of (top) the IMP8 IMF B_Y, (middle) B_Z, and (bottom) solar wind dawn-dusk electric field E_Y are superposed.

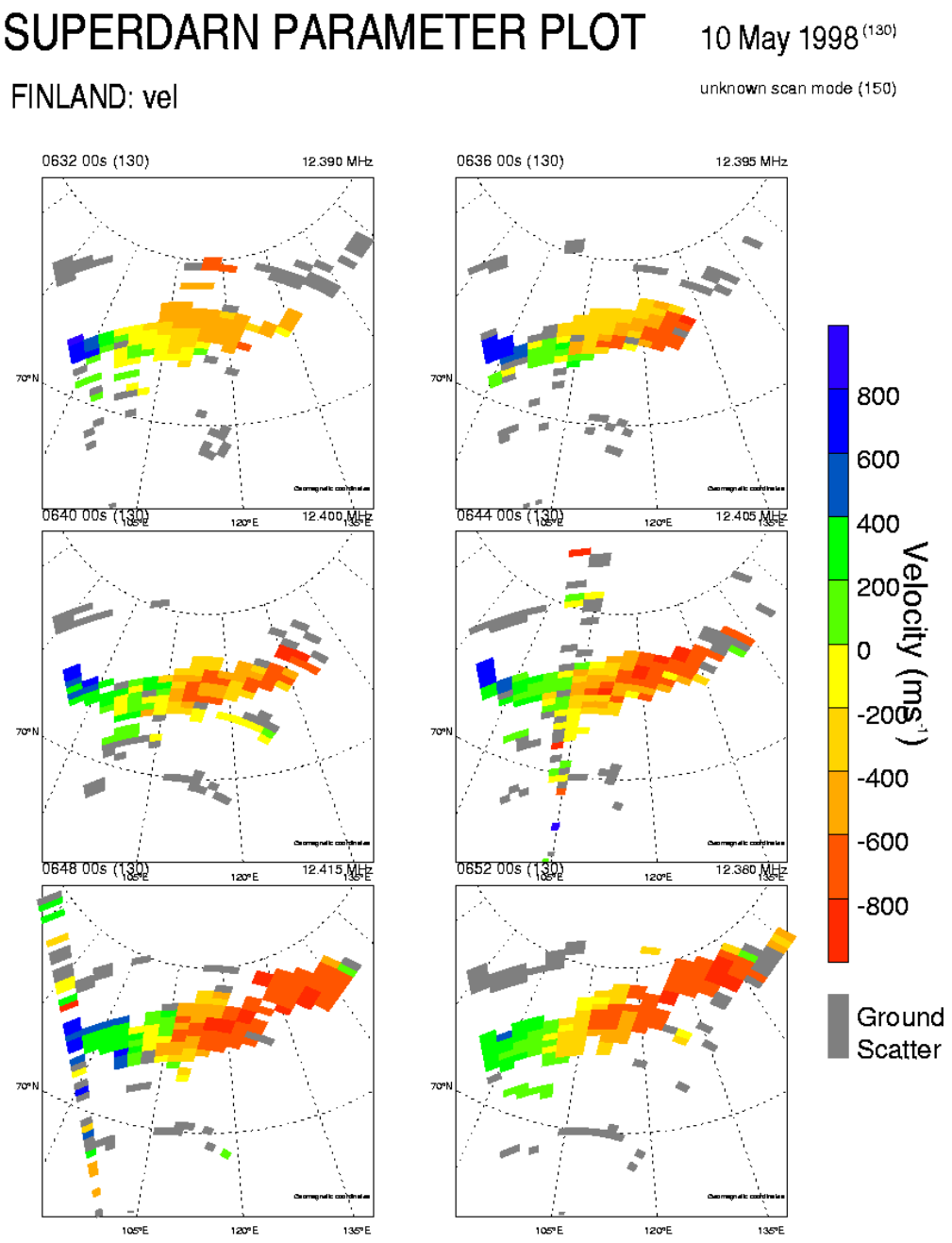

Fig. 6 The Finland radar velocity maps showing a poleward progressing flow channel.

in the cusp footprint that was identified by backscatter associated with large spectral widths (not shown) exceeding 400 m/s between 0530 and 0830 UT. Each consecutive flow burst started at lower latitude as a consequence of intense magnetic flux erosion while the IMF remained strongly southward. For east-west oriented flow channels that are tilted with respect to constant magnetic latitude the observed velocities are l-o-s components of the pulsed northeastward flow in poleward progressing flow channels (Figure 6). Four major flow channels were associated with poleward progressing enhancements of the westward DPY Hall current detected by the IMAGE magnetometer chain (see heavy arrows). For IMF $B_Y < 0$ the cusp is displaced to the pre-noon sector (0700 UT approximately corresponds to about 1000 MLT for beam 9) thus the radar beams observed (within the convection throat) the flows on newly reconnected field lines as they were dragged antisunward and duskward.

The dawn-dusk component of the solar wind Alfvén wave electric field (Figure 5; bottom panel) if imposed on the magnetopause along the X line is expected to modulate the reconnection rate. Assuming that the low latitude edge of the flow burst is the ionospheric signature of the FTE onset at the subsolar magnetopause the reconnection appears to be delayed after the estimated arrival at the magnetopause of the duskward electric field (southward IMF) and then terminated by a dip in generally duskward electric field (or a positive excursion of the IMF B_Z). Since the magnetic tension on the newly opened field lines should be released on Alfvén time scale (< 3 min) after each major reconnection (dawn-dusk electric field) pulse the observed PIF delays suggest that the reconnection onset at the subsolar magnetopause was delayed by several minutes from the arrival of duskward electric field (southward IMF B_Z).

In the above we concentrated on the large scale long-period Alfvénic IMF fluctuations and the ionospheric response but noted the presence of short time scales and a possible link to FLRs. The lower-than-standard temporal resolution radar mode does not allow to examine the correlation with PIFs on scales of minutes or less (apart from a ~8-min structure of the third of the FCEs marked by small arrows in Figures 3b and 5). However, the 10-s IMAGE magnetometer data are often correlated on such short time scales with the IMF measured by IMP 8 (see, e.g., a one-to-one correspondence between the IMP-8 B_Y and NAL X time series just before the first heavy arrow in Figure 3b).

4 Discussion

The correlations of the ground magnetic field and PIFs with the solar wind Alfvén waves suggest that on these occasions the PIFs are driven by solar wind Alfvén waves coupling to the dayside magnetopause. The Alfvén wave dawn-dusk electric field if imposed on the magnetopause along the X line should modulate the reconnection rate into pulses. The ionospheric and ground magnetic signatures of this coupling are consistent with FTE signatures and associated with poleward progressing DPY currents in the cusp footprint.

The time lags of the ionospheric response to solar wind Alfvén waves that were derived from the correlation analysis of the IMF B_Y (or E_Y) and the ground magnetic X component tend to be several minutes longer than the estimated propagation delays. This is significantly more than the expected Alfvén propagation time from the magnetopause to the ionosphere of a few minutes (1-3 min). Similarly, relatively long (~7 min) delays of FTEs after the expected time arrival at the subsolar magnetopause of the southward IMF turning were observed and attributed to the intrinsic time scale for reconnection at the magnetopause by *Russell et al*. [1997]. Also, the latter authors concluded that quasiperiodic FTEs can occur under steady solar wind conditions (see also Le et al., 1993). However, we note that the (17

September, 1979) solar wind data discussed by these authors [*Le et al.,* 1993; their Figure 2] seem to indicate Alfvénic fluctuations that we associate with the FTEs that were observed every 5-6 min by ISEE-1 spacecraft in the magnetosheath. This can be seen more clearly by detrending or filtering the ISEE-3 IMF data while noting a steady IMF magnitude. Adopting the propagation time determined by *Russell et al.* [1997], there is a delay of a few minutes between the expected arrival times of the southward turnings of the solar wind Alfvén wave and the FTEs observed by ISEE 1. This is quite similar to our results showing a delayed appearance of PIF transients in the cusp footprint following the estimated arrival time at the subsolar magnetopause of the Alfvén wave southward turnings.

Recently, the surface-wave-induced magnetic reconnection (SWIMR) mechanism [*Uberoi et al.,* 1996, 1999] has been invoked to explain the observed intrinsic time scale for reconnection [*Russell et al.,* 1997]. This mechanism is based on a concept of resonant absorption of Alfvén waves near a neutral point [*Uberoi,* 1994]. It assumes a source of hydromagnetic surface waves with a broad spectrum of frequencies at the magnetopause; the high-frequency surface waves being responsible for excitation of FLRs and low-frequency surface waves for magnetic reconnection through resonant coupling to the collissionless tearing mode [*Terasawa,* 1983]. Solar wind Alfvén waves and their interaction with the bow shock which generates a set of fast, intermediate (Alfvén) and slow mode waves can provide such source (an external driver for pulsed reconnection). By the same token, it can be envisaged that the low-frequency FLRs (shear Alfvén waves which can couple to slow mode waves [*Bhattacharjee et al.*, 1999]) excited on the field lines adjacent to the dayside magnetopause could provide a resonant surface on the inside neutral boundary and thus a magnetospheric feedback to the reconnection region [*Prikryl et al.*, 1998] by being resonantly absorbed near the neutral point [*Uberoi,* 1994]. This notion is consistent with the Taylor model [*Hahm and Kulsrud*, 1985] of forced reconnection, a reconnection induced by perturbing the boundary of a simple slab equilibrium of an incompressible plasma with a resonant surface inside. The correspondence between the forced reconnection model and SWIMR has been noted by *Uberoi and Zweibel* [1999] who showed that "the theory of forced reconnection is actually embedded in the Alfvén resonance theory".

5 Conclusions

Pulsed ionospheric flows (PIFs) that are believed to be ionospheric signatures of flux transfer events (FTEs) in the cusp footprint are correlated with the solar wind Alfvén waves observed by ISTP satellites. The long and short period PIFs observed by the CUTLASS SuperDARN radar and supported by the IMAGE ground magnetometer data are correlated with the IMF upstream of the bow shock. It is concluded that the dayside reconnection was pulsed by the dawn-dusk component of the Alfvén wave electric field (external driver) modulating the reconnection rate as evidenced by the radar observations. The standard estimates of the propagation time between the spacecraft and the subsolar magnetopause are found to be several minutes shorter than the correlation lags between the solar wind magnetic (B_Z–) or electric (E_Y+) field pulses and PIFs confirming previous finding [*Russell et al.,* 1997] that the reconnection at the magnetopause may not occur immediately after the southward IMF (duskward electric field) arrives at the magnetopause. The theory of resonant absorption of Alfvén surface waves near a neutral point [Uberoi, 1994] and the link between forced reconnection and Alfvén resonance theory [*Uberoi and Zweibel,* 1999] suggest similar time delays of the reconnection onset.

Acknowledgements. CUTLASS SuperDARN radar is supported by the Particle Physics and Astronomy

Research Council (PPARC), UK, the Swedish Institute for Space Physics, Uppsala, and the Finnish Meteorological Institute, Helsinki. The IMAGE magnetometer data used in this paper were collected as a German-Finnish-Norwegian-Polish project conducted by the Technical University of Braunschweig. We acknowledge contributions by principal investigators of the ACE, IMP8, and WIND instruments, namely, E. Stone (Advanced Composition Explorer), A. Lazarus (Plasma Instrument), R. Lepping (Magnetic Field Investigation), and R. Lin (Three-Dimensional Plasma Analyzer).

References

Bhattacharjee, A., C.A. Kletzig, Z.W. Ma, C.S. Ng, N.F. Otani, and X. Wang, Four-field model for dispersive field-line resonances: Effects of coupling between shear-Alfvén and slow modes, Geophys. Res. Lett., 26, 3281-3284, 1999.

Belcher, J.W., and L. Davis, Jr., Large-amplitude Alfvén waves in the interplanetary medium, 2, *J. Geophys. Res.*, **76**, 3534-3563, 1971.

Berchem, J., and C.T. Russell, Flux transfer events on the magnetopause: Spatial distribution and controlling factors, *J. Geophys. Res.*, **89**, 6689-6703, 1984.

Cable, S., and Y. Lin, MHD simulations pf oppositely propagating Alfvén waves in the magnetosheath and solar wind, *Geophys. Res. Lett.*, **25**, 1821-1824, 1998.

Cowley, S.W.H, M.P. Freeman, M. Lockwood, and M.F. Smith, The ionospheric signatures of flux transfer events, Eur. Space Agency Spec. Publ., ESA SP-330, 105-112, 1991.

Cowley, S.W.H, and M. Lockwood, Excitation and decay of solar-wind driven flows in the magnetosphere-ionosphere system, *Annales Geophys.*, **10**, 103-115, 1992.

Dungey, J.W., Interplanetary magnetic field and the auroral zones, *Phys. Rev. Lett.*, **6**, 47, 1961.

Fairfield, D. H., Averaged and unusual locations of the Earth's magnetopause and bow shock, *J. Geophys. Res*., **76**, 6700-6716, 1971.

Goertz, C.K., E. Nielsen, A. Korth, K.H. Glassmeier, C. Haldoupis, P. Hoeg, and D. Hayward, Observations of a possible ground signature of flux transfer events, *J. Geophys. Res*., **90**, 4069-4078, 1985.

Greenwald, R.A., K.B. Baker, J.R. Dudeney, M. Pinnock, T.B. Jones, E.C. Thomas, J.-C. Villain, J.-C. Cerrisier, C. Senior, C. Hanuise, R.D. Hunsucker, G. Sofko, J. Koehler, E. Nielsen, R. Pellinen, A.D.M. Walker, N. Sato, and H. Yamagishi, DARN/SUPERDARN A global view of the dynamics of high-latitude convection, *Space Sci. Rev.*, **71**, 761-796, 1995.

Hahm, T.S., and R.M. Kulsrud, Forced magnetic reconnection, *Phys. Fluids,* **28** (8), 2412-2418, 1985.

Kuo, H., C.T. Russell, and G. Lee, Statistical studies of flux transfer events, *J. Geophys. Res.*, **100**, 3513-3519, 1995.

Lester, M., O. de la Beaujardière, J.C. Foster, M.P. Freeman, H. Lühr, J.M. Ruohoniemi, and W. Swider, The response of the large scale ionospheric convection pattern to changes in the IMF and substorms: results from the SUNDIAL 1987 campaign, *Ann. geophys.*, **11**, 556-571, 1993.

Le, G., C.T. Russell, and H. Kuo, Flux transfer events: Spontaneous or driven?, *Geophys. Res. Lett.*, **20**, 791-794, 1993.

Lin, Y., L.C. Lee, and M. Yan, Generation of dynamic pressure pulses downstream of the bow shock by variations in the interplanetary magnetic field orientation, *J. Geophys. Res.*, **101**, 479-493, 1996.

Lockwood, M., and M.N. Wild, On the quasi-periodic nature of magnetopause flux transfer events, *J.*

Geophys. Res., **98**, 5935-5940, 1993.
Lockwood, M., P.E. Sandholt, S.W.H. Cowley, and T. Oguti, Interplanetary magnetic field control of dayside auroral activity and the transfer of momentum across the dayside magnetopause, *Planet. Space Sci.*, **67**, 1347-1365, 1989.
Lockwood, M., W.F. Denig, A.D. Farmer, V.N. Davda, S.W.H. Cowley, and H. Luhr, Ionospheric signatures of pulsed reconnection at the Earth's magnetopause, *Nature*, **361**, 424-428, 1993.
Nishitani, N., T. Ogawa, M. Pinnock, M.P. Freeman, J.R. Dudeney, J.-P. Villain, K.B. Baker, N. Sato,, H. Yamagishi, and H. Matsumoto, A very large scale flow burst observed by the SuperDARN radars, *J. Geophys. Res.*, **104**, 22469-22486, 1999.
Ogilvie, K.W. and G.K. Parks, First results from WIND spacecraft, *Geophys. Res. Lett.,* **23**, 1179-1181, 1996.
Øieroset, M., P.E. Sandholt, H. Lühr, W.F. Denig, and T. Moretto, Auroral and geomagnetic events at cusp/mantle latitudes in the prenoon sector during positive IMF By conditions:Signatures of pulsed magnetopause reconnection, *J. Geophys. Res.*, **102**, 7191-7205, 1997.
Paschmann, G., et al., Plasma acceleration at the Earth's magnetopause: Evidence for reconnection, *Nature*, **282**, 243, 1979.
Pinnock, M., A.S. Rodger, J.R. Dudeney, F. Rich and K.B. Baker, High spatial and temporal resolution observations of the ionospheric cusp, *Ann. Geophys.,* **13**, 919-925, 1995.
Prikryl, P., R.A. Greenwald, G.J. Sofko, J.P. Villain, and C.W.S. Ziesolleck, and E. Friis-Christensen, Solar-wind driven pulsed magnetic reconnection at the dayside magnetopause, Pc5 compressional oscillations, and field line resonances, *J. Geophys. Res.*, **103**, 17307-17322, 1998.
Prikryl, P., J.W. MacDougall, I.F. Grant, D.P. Steele, G.J. Sofko, and R.A. Greenwald, Observations of polar patches generated by solar wind Alfvén wave coupling to the dayside magnetosphere, *Ann. Geophys.*, **17**, 463-489, 1999.
Provan, G., T.K. Yeoman, and S.E. Milan, CUTLASS Finland radar observations of the ionospheric signatures of flux transfer events and the resulting plasma flows, *Ann. Geophys.*, **16**, 1411-1422, 1998.
Richardson, J.D., and K.I. Paularena, The orientation of plasma structure in the solar wind, *Geophys. Res. Lett.*, **25**, 2097-2100, 1998.
Rijnbeek, R.P., S.W.H. Cowley, D.J. Southwood,, and C.T. Russell, A survey of dayside flux transfer events observed by ISEE 1 and 2, *J. Geophys. Res.*, **89**, 786-800, 1984.
Roelof, E.C., and D.G. Sibeck, Magnetopause shape as a bivariate function of interplanetary magnetic field B_z and solar wind dynamic pressure, *J. Geophys. Res.*, **98**, 21421-21450, 1993.
Russell, C.T., The configuration of the magnetosphere, in *Critical Problems of Magnetospheric Physics,* Ed E.R. Dyer, NSF, Washington, D. C., 1972.
Russell, C.T., and R.L. McPherron, The magnetotail and substorms, *Space Sci. Rev.*, **15**, 205, 1973.
Russell, C.T., and R.C. Elphic, Initial ISEE magnetometer results: Magnetopause observations, *Space Sci. Rev.*, **22**, 681-715, 1978.
Russell, C.T., and R.C. Elphic, ISEE observations of flux transfer events at the dayside magnetopause, *Geophys. Res. Lett.*, **6**, 33, 1979.
Russel, C.T., G. Le, H. Kawano, S.M. Petrinec, and T.L. Zhang, Intrinsic time scale for reconnection on the dayside magnetopause, *Adv. Space Res.,* **19**, 1913-1917, 1997.
Sandholt, P.E., M. Lockwood, T. Oguti, S.W.H. Cowley, K.S.C. Freeman, B. Lebekk, A. Egeland, and

D.M. Willis, Midday auroral breakup events and related energy and momentum transfer from the magnetosheath, *J. Geophys. Res.*, **95**, 1039-1060, 1990.

Sibeck, D.G., K. Takahashi, S. Kokubun, T. Mukai, K.W. Ogilvie, and A. Szabo, A case study of oppositely propagating Alfvénic fluctuations in the solar wind and magnetosheath, *Geophys. Res. Lett.*, **24**, 3133-3136, 1997.

Sibeck, D.G., T.-D. Phan, R.P. Lin, R.P. Lepping, T. Mukai, and S. Kokubun, A survey of MHD waves in the magnetosheath: International Solar Terrestrial Program observations, *J. Geophys. Res.*, **105**, 129-137, 2000.

Smith, C. W., M. H. Acuna, L. F. Burlaga, J. L'Heureux, N. F. Ness and J. Scheifele, The ACE Magnetic Field Experiment, Space Science Reviews, 86, 613-632, 1999.

Stauning, P., C.R. Clauer, T.J. Rosenberg, E. Friis-Christensen, and R. Sitar, Observations of solar-wind-driven progression of interplanetary magnetic field By-related dayside ionospheric disturbances, *J. Geophys. Res.*, **100**, 7567-7585, 1995.

Terasawa, T., Hall current effect on tearing mode instability, *Geophys. Res. Lett.*, **10**, 475, 1983.

Uberoi, C., Resonant absorption of Alfvén waves near a neutral point, *J. Plasma Phys.,* **52**, 215-221, 1994.

Uberoi, C., L.J. Lanzerotti, and A. Wolfe, Surface waves and magnetic reconnection at a magnetopause, *J. Geophys. Res.*, **101**, 24979-24983, 1996.

Uberoi, C., L.J. Lanzerotti, and C.G. Maclennan, Remarks on the intrinsic timescale for reconnection on the dayside magnetopause, *J. Geophys. Res.*, **104**, 25153-25157, 1999.

Uberoi, C., and E.G. Zweibel, Alfvén resonances and forced reconnection, *J. Plasma Phys.*, **62** (3), 345-350, 1999.

Van Eyken, A.P., H Rishbeth, D.M. Willis, and S.W.H. Cowley, Initial EISCAT observations of plasma convection at invariant latitudes 70^{o}-77^{o}, *J. Atmos. Terr. Phys.*, **46**, 635-641, 1984.

Viljanen, A. and L. Häkkinen, IMAGE magnetometer network, in *Satellite-ground based coordination sourcebook*, Eds. M. Lockwood, M.N. Wild and H.J. Opgenoorth, ESA publications SP-1198, 111-117, 1997.

Vorobjev, V.G., G. Gustafsson, G.V. Starkov, Y.I. Feldstein, and N.F. Shevnina, Dynamics of day and night aurora during substorms, *Planet., Space Sci.*, **23**, 269-278, 1975.

Table 1 The maximum correlation coefficient and mean lag between the spacecraft

Spacecraft pair	Time UT	IMF B_Y CC, lag (min)	B_Z CC, lag (min)
WI-I8	0430-0830	0.91, +47	0.88, +46
ACE-I8	0430-0830	0.87, +37	0.71, +40
ACE-WI	0430-0830	0.79, +11	0.65, +8

Table 2 The propagation delays (min)

Date/ spacecraft	Estimated (s/c to MP)	Observed (s/c to ionosphere) (IMF B_Y, X)	(E_Y or -B_Z, X)
IMP 8	4 ± 3	19 ± 1	16 ± 1
ACE	42 ± 3	58 ± 2	57 ± 2
WIND	50 ± 3	66 ± 1	63 ± 1